

Supplement of Atmos. Chem. Phys., 21, 3215–3234, 2021
<https://doi.org/10.5194/acp-21-3215-2021-supplement>
© Author(s) 2021. This work is distributed under
the Creative Commons Attribution 4.0 License.



Supplement of

Effects of marine fuel sulfur restrictions on particle number concentrations and size distributions in ship plumes in the Baltic Sea

Sami D. Seppälä et al.

Correspondence to: Sami D. Seppälä (sami.seppala@fmi.fi)

The copyright of individual parts of the supplement might differ from the CC BY 4.0 License.

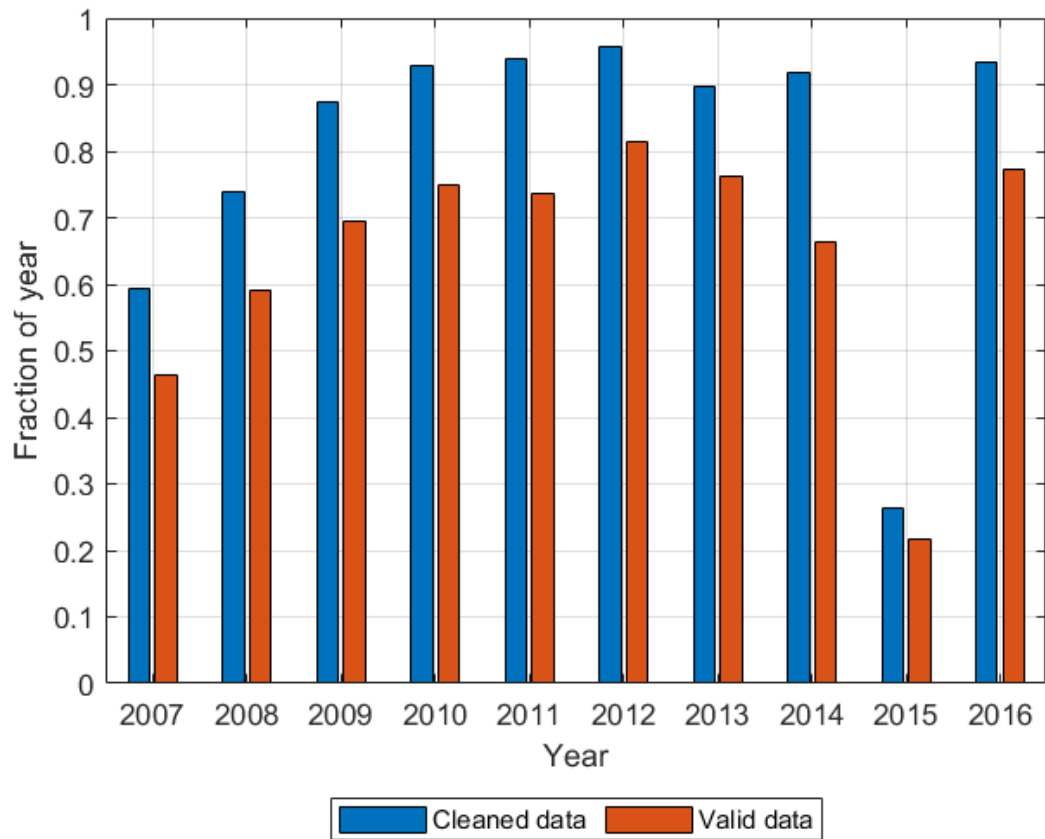
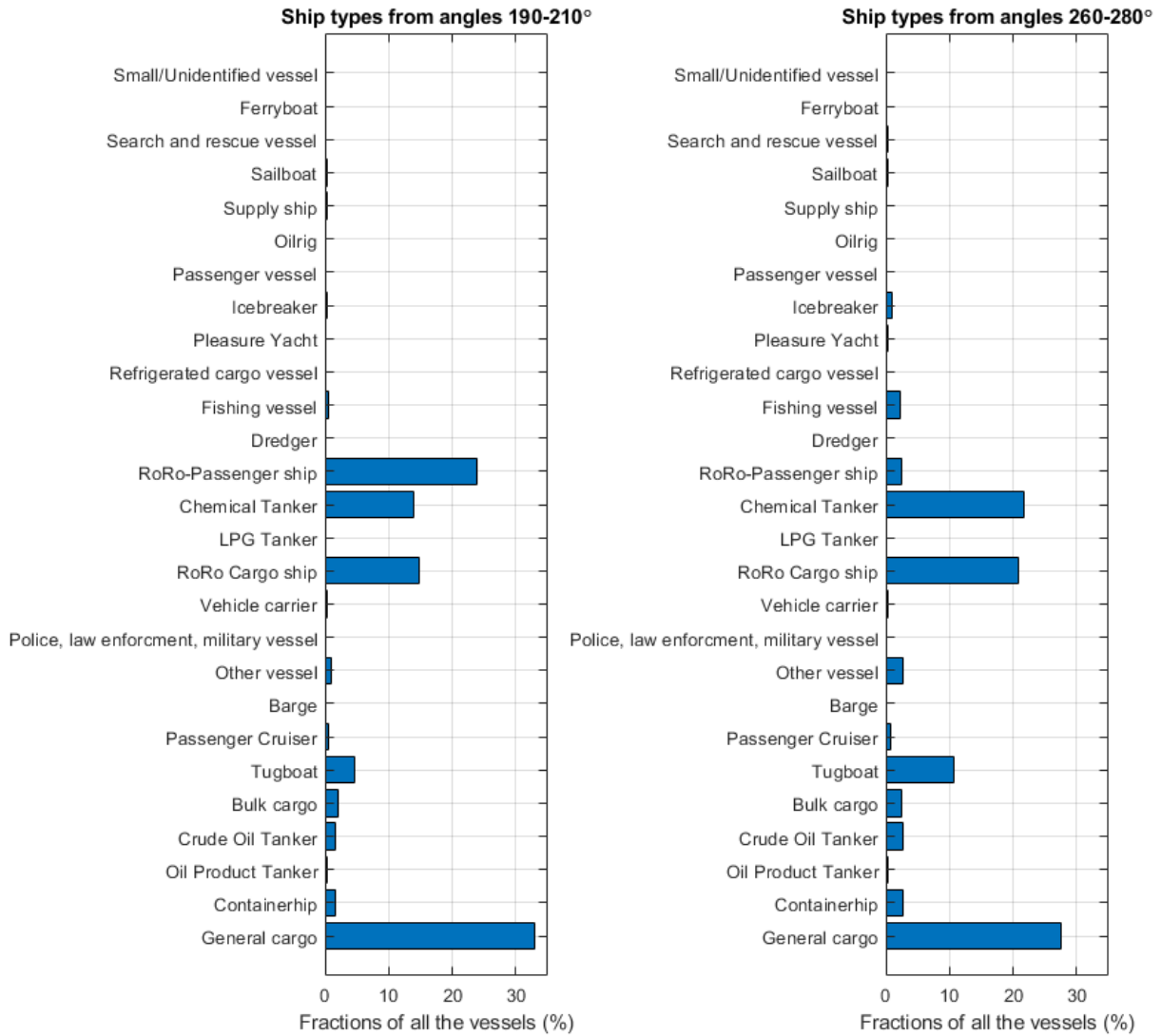


Figure S1: Coverages of cleaned and valid periods of the DMPS data for each year (2007-2016).



5 **Figure S2: Fractions (%) of different ship types from angles 190-210° and 260-280°. LNG and RoRo stand for liquefied petroleum gas and Roll on roll of, respectively.**

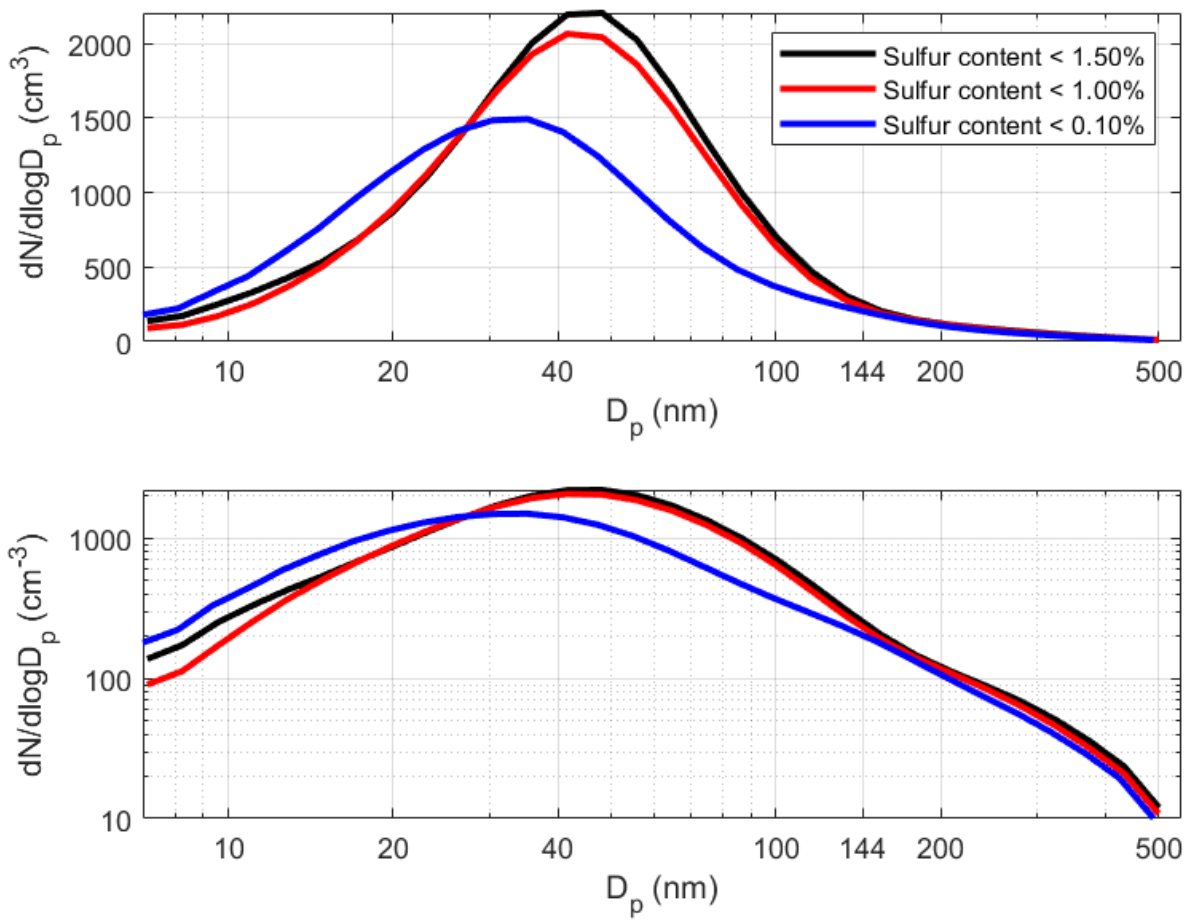
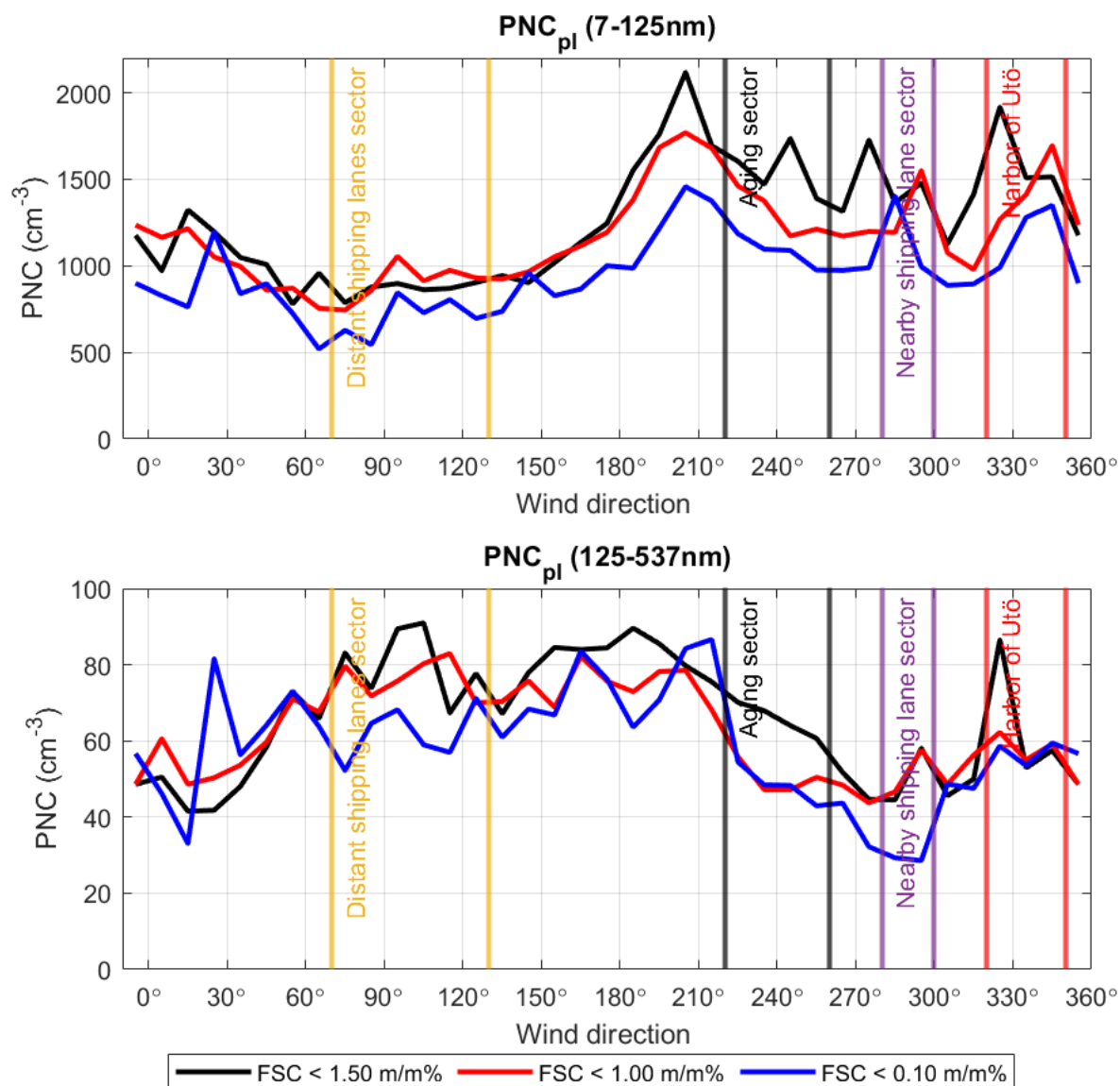


Figure S3: Average number size distributions of the valid plumes (NSD_{pl}) during the different fuel sulfur content (FSC) restrictions.



10 **Figure S4:** Average particle number concentrations of the plume particles (PNC_{pl}) in size range 7-125 nm (upper panel) and 125-537 nm (lower panel) for different FSC restrictions averaged for 10°-sectors. Distant shipping lanes sector, ageing sector, nearby shipping lane sector, and harbor of Utö are marked with vertical line pairs.

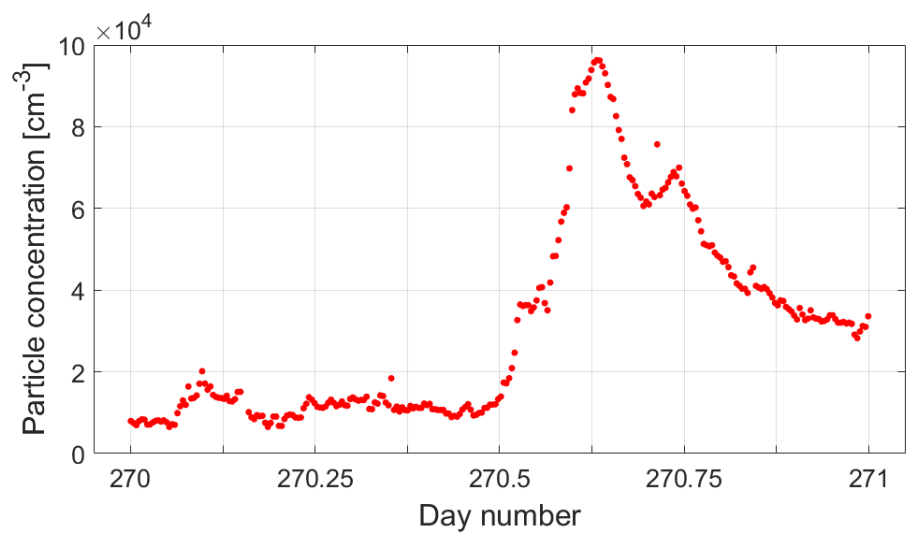
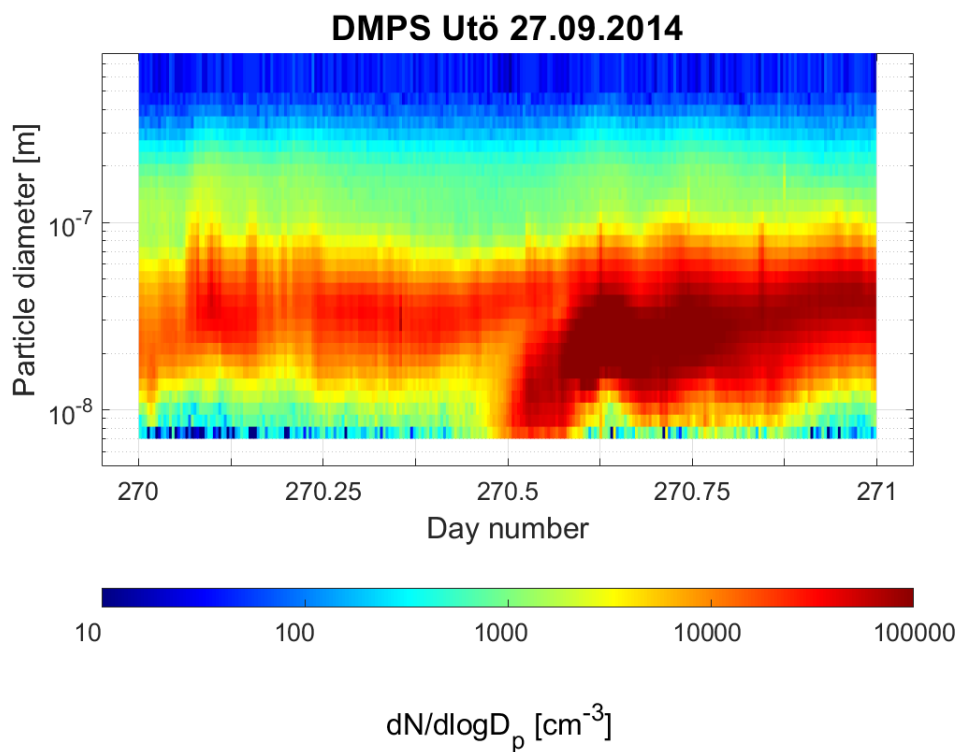
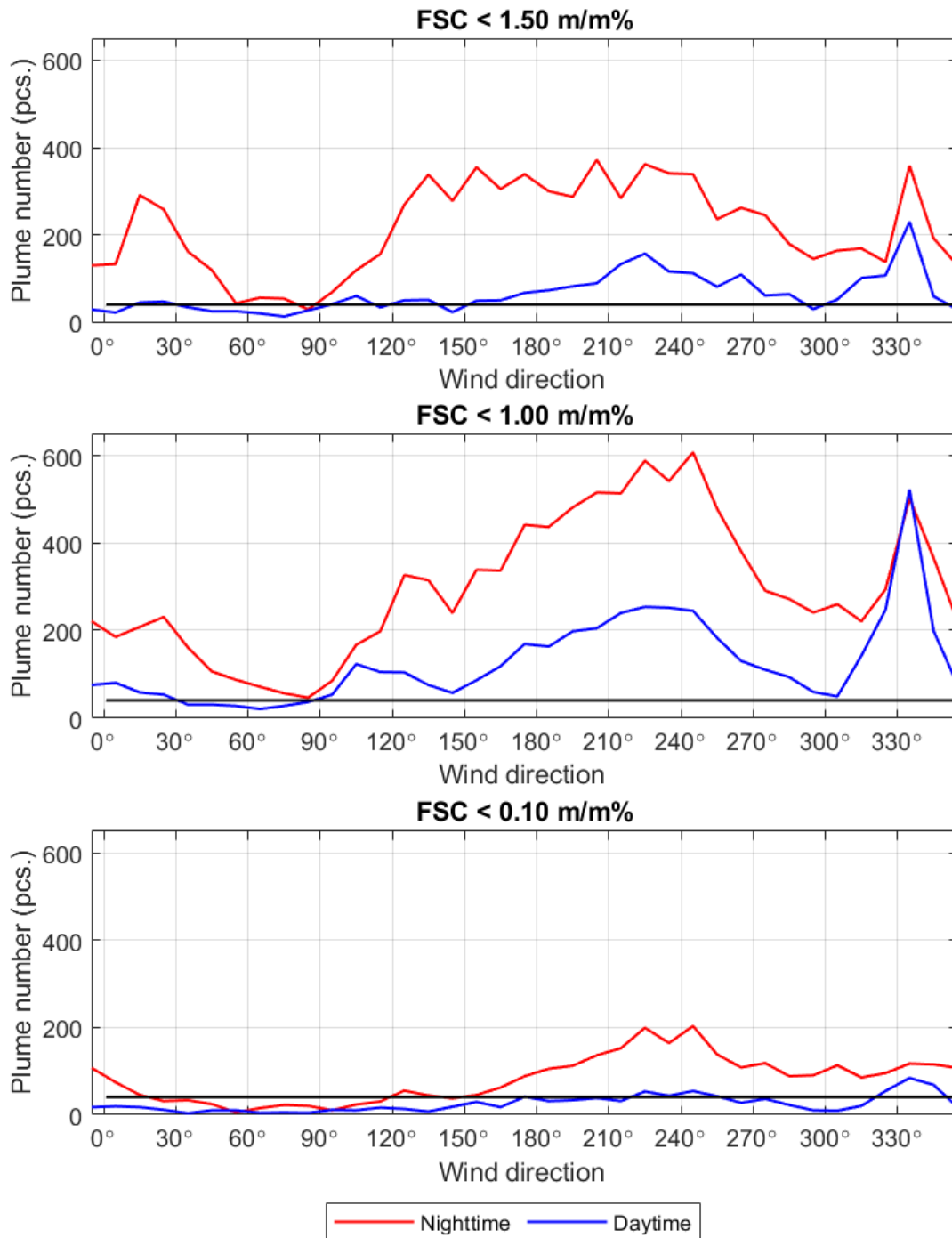


Figure S5: An example size distribution (upper) and particle concentration (below) of intense nucleation event in 2014.



15 **Figure S6: Average number of plumes during $I_{\text{tot}} < 0$ (nighttime) and $I_{\text{tot}} > 200 \text{ W m}^{-2}$ (daytime) during different FSC restrictions as a function of wind direction. The black line marks the limit of 40 observed plumes per 10° sectors.**

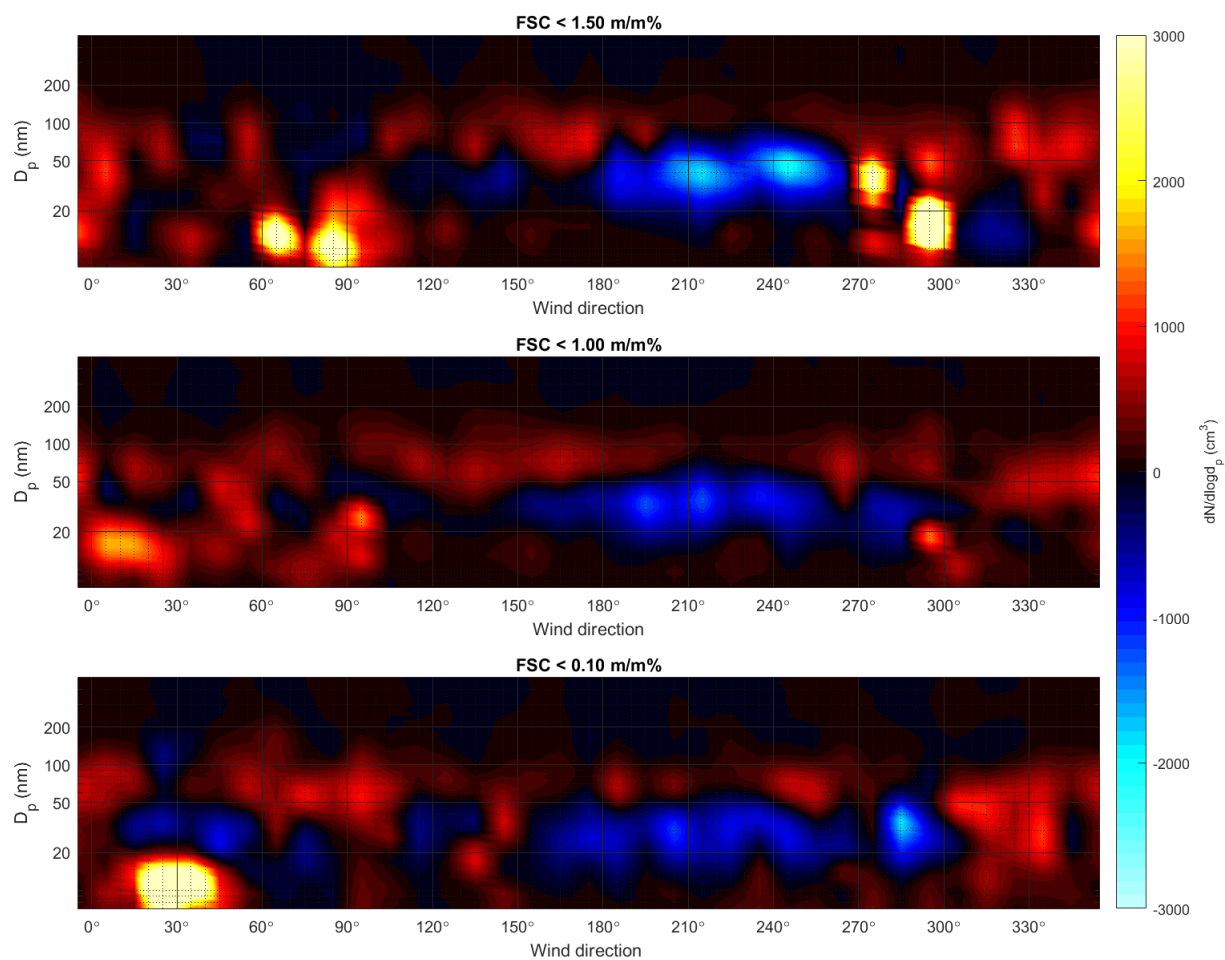
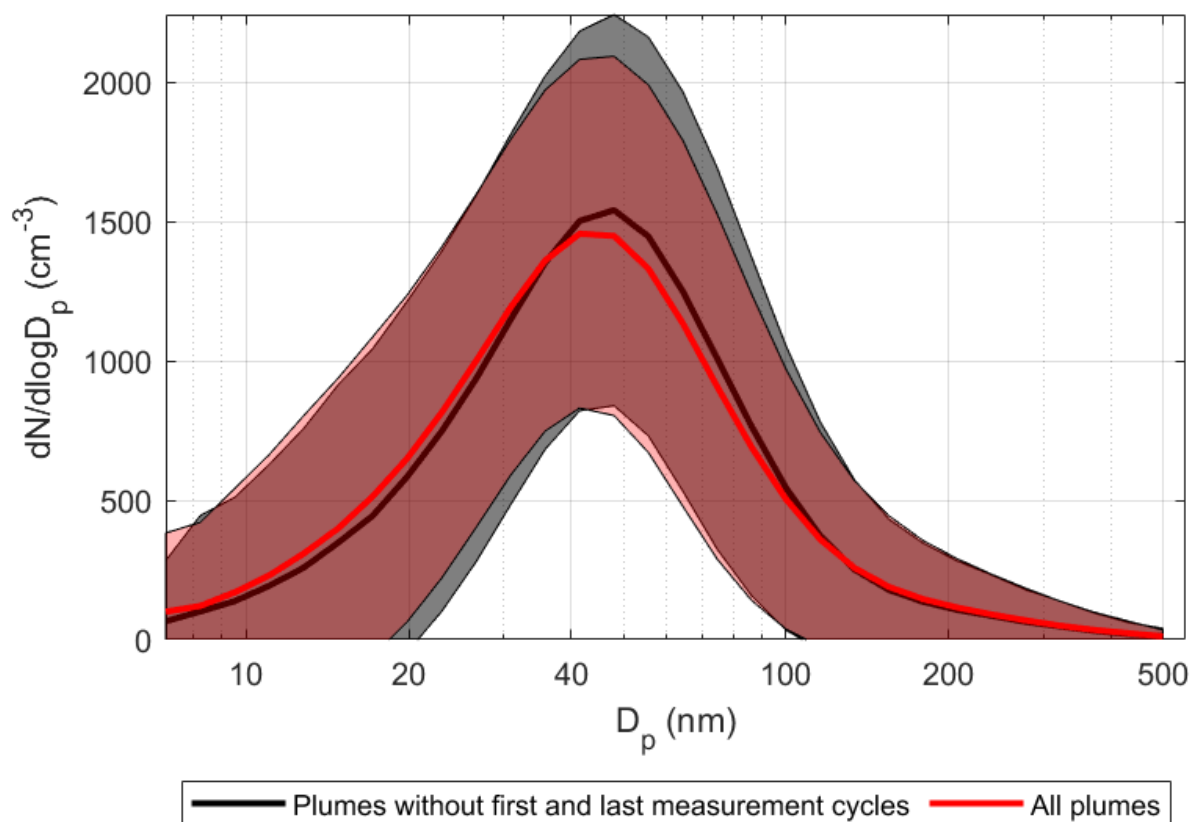


Figure S6: Average change caused to NSD_p by sunlight from different wind directions during the different FSC restrictions



20 **Figure S7: Average NSD_{pl} of all the plumes and all the plumes with the last and first measurement cycles removed (also plumes with only one measurement cycle removed). Individual NSD_{pl} have been normalized to a total concentration of 1000 cm⁻³.**

Error caused by lengthy measurement cycles of the DMPS

Because of the relatively long measurement cycle of the DMPS (5 min 20 s), 36.4% of the measured plumes were shorter than one measurement cycle and 63.8 % were maximum of two measurement cycles long. Also, for the rest of the plumes, every plume has to have ended and started during the last and first measurement cycles. This causes an error to PNC_{pl} and NSD_{pl} of an individual plume as the whole NSD_{pl} is not measured during these cycles. As the particle sizes are scanned from small particles to large, in the first cycle the small particles of the NSD_{pl} are not measured and during the last measurement cycle, the large particles of the NSD_{pl} are not measured. This also causes error in correcting multiply charged particles, as,

25

during the first measurement cycle, only the PNC_{pl} of the larger particles is measured. Therefore, a large fraction of the measured PNC_{ppt} of smaller particles is considered as multiply charged large particles, and the PNC_{pl} of small particles is decreased even further. During the last measurement cycle, the PNC_{pl} is vice versa overestimated for the smaller particles as the low PNC_{pl} of the large particles causes a too low estimate for the number of double-charged particles measured at the smaller particle sizes, which falsely increases the PNC_{pl} of small particles. However, as these effects are opposite and counteract each other, the rather large data set renders the error to be small after the statistical analysis. The inversion routines of the DMPS are discussed in more detail in (Pfeifer et al., 2014). To estimate the error caused by the first and last measurement cycles, NSD_{pl} were drawn for all plumes and the plumes with the last and first measurement cycles removed. These are presented in the supplemental material (Fig. S8). The comparison shows that the influence of the first and last measurement cycles is not significant.

40 **References**

Pfeifer, S., Birmili, W., Schladitz, A., Müller, T., Nowak, A., and Wiedensohler, A.: A fast and easy-to-implement inversion algorithm for mobility particle size spectrometers considering particle number size distribution information outside of the detection range, *Atmos. Meas. Tech.*, 7(1), 95–105, <https://doi.org/10.5194/amt-7-95-2014>, 2014.

45